EUROPEAN ORGANIZATION FOR NUCLEAR RESEARCH

CERN-PPE/94-210

19 December 1994

Observation of Orbitally Excited B Mesons

DELPHI Collaboration

Abstract

Experimental evidence for the existence of orbitally excited B meson states is presented in an analysis of the $B\pi$ and $B^*\pi$ distribution of $Q = m(B^{**}) - m(B^{(*)}) - m(\pi)$ using Z^0 decay data taken with the DELPHI detector at LEP. The mean Q-value of the decays $B^{**} \to B^{(*)}\pi$ is measured to be $284 \pm 5\,(\text{stat.}) \pm 15\,(\text{syst.})$ MeV/c^2, and the Gaussian width of the signal is $79 \pm 5\,(\text{stat.}) \pm 8\,(\text{syst.})$ MeV/c^2. This signal can be described as a single resonance of mass $m = 5732 \pm 5\,(\text{stat.}) \pm 20\,(\text{syst.})$ MeV/c^2 and full width $\Gamma = 145 \pm 28$ MeV/c^2. The observed shape is also consistent with the production of several broad and narrow states as predicted by the quark model and partly observed in the D-meson sector. The production rate of B^{**} per b-jet is found to be $0.27 \pm 0.02\,(\text{stat.}) \pm 0.06\,(\text{syst.})$.

(To be submitted to Physics Letters B)

P.Abreu[21], W.Adam[8], T.Adye[38], E.Agasi[31], I.Ajinenko[43], R.Aleksan[40], G.D.Alekseev[15], P.P.Allport[22], S.Almehed[24], F.M.L.Almeida[48], S.J.Alvsvaag[4], U.Amaldi[8], S.Amato[48], A.Andreazza[28], M.L.Andrieux[13], P.Antilogus[25], W-D.Apel[16], Y.Arnoud[40], B.Åsman[45], J-E.Augustin[19], A.Augustinus[31], P.Baillon[8], P.Bambade[19], F.Barao[21], R.Barate[13], G.Barbiellini[47], D.Y.Bardin[15], G.J.Barker[35], A.Baroncelli[41], O.Barring[8], J.A.Barrio[26], W.Bartl[51], M.J.Bates[38], M.Battaglia[14], M.Baubillier[23], J.Baudot[40], K-H.Becks[53], M.Begalli[37], P.Beilliere[7], Yu.Belokopytov[8], P.Beltran[10], A.C.Benvenuti[5], M.Berggren[42], D.Bertrand[2], F.Bianchi[46], M.Bigi[46], M.S.Bilenky[15], P.Billoir[23], J.Bjarne[24], D.Bloch[9], M.Blume[53], S.Blyth[35], V.Bocci[39], T.Bolognese[40], M.Bonesini[28], W.Bonivento[28], P.S.L.Booth[22], G.Borisov[43], C.Bosio[41], B.Bostjancic[44], S.Bosworth[35], O.Botner[49], B.Bouquet[19], C.Bourdarios[19], T.J.V.Bowcock[22], M.Bozzo[12], P.Branchini[41], K.D.Brand[36], R.A.Brenner[14], H.Briand[23], C.Bricman[2], L.Brillault[23], R.C.A.Brown[8], P.Bruckman[17], J-M.Brunet[7], L.Bugge[33], T.Buran[33], A.Buys[8], M.Caccia[28], M.Calvi[28], A.J.Camacho Rozas[42], T.Camporesi[8], V.Canale[39], M.Canepa[12], K.Cankocak[45], F.Cao[2], F.Carena[8], P.Carrilho[48], L.Carroll[22], C.Caso[12], V.Cassio[46], M.V.Castillo Gimenez[50], A.Cattai[8], F.R.Cavallo[5], L.Cerrito[39], V.Chabaud[8], A.Chan[1], Ph.Charpentier[8], L.Chaussard[25], J.Chauveau[23], P.Checchia[36], G.A.Chelkov[15], P.Chliapnikov[43], P.Chochula[6], V.Chorowicz[8], J.T.M.Chrin[50], V.Cindro[44], P.Collins[8], J.L.Contreras[19], R.Contri[12], E.Cortina[50], G.Cosme[19], F.Cossutti[47], H.B.Crawley[1], D.Crennell[38], G.Crosetti[12], J.Cuevas Maestro[34], S.Czellar[14], E.Dahl-Jensen[29], J.Dahm[53], B.Dalmagne[19], M.Dam[33], G.Damgaard[29], A.Daum[16], P.D.Dauncey[38], M.Davenport[8], W.Da Silva[23], C.Defoix[7], G.Della Ricca[47], P.Delpierre[27], N.Demaria[35], A.De Angelis[8], H.De Boeck[2], W.De Boer[16], S.De Brabandere[2], C.De Clercq[2], M.D.M.De Fez Laso[50], C.De La Vaissiere[23], B.De Lotto[47], A.De Min[28], L.De Paula[48], C.De Saint-Jean[40], H.Dijkstra[8], L.Di Ciaccio[39], F.Djama[9], J.Dolbeau[7], M.Donszelmann[8], K.Doroba[52], M.Dracos[9], J.Drees[53], K.-A.Drees[53], M.Dris[32], Y.Dufour[7], F.Dupont[13], D.Edsall[1], R.Ehret[16], T.Ekelof[49], G.Ekspong[45], M.Elsing[53], J-P.Engel[9], N.Ershaidat[23], M.Espirito Santo[21], D.Fassouliotis[32], M.Feindt[8], A.Fenyuk[43], A.Ferrer[50], T.A.Filippas[32], A.Firestone[1], H.Foeth[8], E.Fokitis[32], F.Fontanelli[12], F.Formenti[8], J-L.Fousset[27], B.Franek[38], P.Frenkiel[7], D.C.Fries[16], A.G.Frodesen[4], R.Fruhwirth[51], F.Fulda-Quenzer[19], H.Furstenau[8], J.Fuster[8], D.Gamba[46], M.Gandelman[18], C.Garcia[50], J.Garcia[42], C.Gaspar[8], U.Gasparini[36], Ph.Gavillet[8], E.N.Gazis[32], D.Gele[9], J-P.Gerber[9], D.Gillespie[8], R.Gokieli[52], B.Golob[44], J.J.Gomez Y Cadenas[8], G.Gopal[38], L.Gorn[1], M.Gorski[52], V.Gracco[12], F.Grard[2], E.Graziani[41], G.Grosdidier[19], P.Gunnarsson[45], J.Guy[38], U.Haedinger[16], F.Hahn[53], M.Hahn[16], S.Hahn[53], S.Haider[31], Z.Hajduk[17], A.Hakansson[24], A.Hallgren[49], K.Hamacher[53], W.Hao[31], F.J.Harris[35], V.Hedberg[24], R.Henriques[21], J.J.Hernandez[50], J.A.Hernando[50], P.Herquet[2], H.Herr[8], T.L.Hessing[8], E.Higon[50], H.J.Hilke[8], T.S.Hill[1], S-O.Holmgren[45], P.J.Holt[35], D.Holthuizen[31], P.F.Honore[7], M.Houlden[22], J.Hrubec[51], K.Huet[2], K.Hultqvist[45], P.Ioannou[3], J.N.Jackson[22], R.Jacobsson[45], P.Jalocha[17], R.Janik[6], G.Jarlskog[24], P.Jarry[40], B.Jean-Marie[19], E.K.Johansson[45], L.Jonsson[24], P.Juillot[9], M.Kaiser[16], G.Kalmus[38], F.Kapusta[23], M.Karlsson[45], E.Karvelas[10], S.Katsanevas[3], E.C.Katsoufis[32], R.Keranen[14], B.A.Khomenko[15], N.N.Khovanski[15], B.King[22], N.J.Kjaer[29], H.Klein[8], A.Klovning[4], P.Kluit[31], J.H.Koehne[16], B.Koene[31], P.Kokkinias[10], M.Koratzinos[8], V.Kostioukhine[43], C.Kourkoumelis[3], O.Kouznetsov[12], P.-H.Kramer[53], M.Krammer[51], C.Kreuter[16], J.Krolikowski[52], I.Kronkvist[24], Z.Krumstein[15], W.Krupinski[17], P.Kubinec[6], W.Kucewicz[17], K.Kulka[49], K.Kurvinen[14], C.Lacasta[50], I.Laktineh[25], C.Lambropoulos[10], J.W.Lamsa[1], L.Lanceri[47], D.W.Lane[1], P.Langefeld[53], V.Lapin[43], I.Last[22], J-P.Laugier[40], R.Lauhakangas[14], G.Leder[51], F.Ledroit[13], V.Lefebure[2], C.K.Legan[1], R.Leitner[30], Y.Lemoigne[40], J.Lemonne[2], G.Lenzen[53], V.Lepeltier[19], T.Lesiak[36], R.Lindner[53], A.Lipniacka[19], I.Lippi[36], B.Loerstad[24], M.Lokajicek[11], J.G.Loken[35], A.Lopez-Fernandez[8], M.A.Lopez Aguera[42], D.Loukas[10], J.J.Lozano[50], P.Lutz[40], L.Lyons[35], G.Maehlum[16], J.Maillard[7], A.Maio[21], A.Maltezos[10], V.Malychev[15], F.Mandl[51], J.Marco[42], B.Marechal[48], M.Margoni[36], J-C.Marin[8], C.Mariotti[41], A.Markou[10], T.Maron[53], C.Martinez-Rivero[42], F.Martinez-Vidal[50], S.Marti i Garcia[50], F.Matorras[42], C.Matteuzzi[28], G.Matthiae[39], M.Mazzucato[36], M.Mc Cubbin[8], R.Mc Kay[1], R.Mc Nulty[22], J.Medbo[49], C.Meroni[28], W.T.Meyer[1], M.Michelotto[36], E.Migliore[46], I.Mikulec[51], L.Mirabito[25], W.A.Mitaroff[51], U.Mjoernmark[24], T.Moa[45], R.Moeller[29], K.Moenig[8], M.R.Monge[12], P.Morettini[12], H.Mueller[16], W.J.Murray[38], B.Muryn[17], G.Myatt[35], F.Naraghi[13], F.L.Navarria[5], S.Navas[50], P.Negri[28], S.Nemecek[11], W.Neumann[53], N.Neumeister[51], R.Nicolaidou[3], B.S.Nielsen[29], V.Nikolaenko[25], P.Niss[45], A.Nomerotski[36], A.Normand[35], W.Oberschulte-Beckmann[16], V.Obraztsov[43], A.G.Olshevski[15], R.Orava[14], K.Osterberg[14], A.Ouraou[40], P.Paganini[19], M.Paganoni[28], P.Pages[9], R.Pain[23], H.Palka[17], Th.D.Papadopoulou[32], L.Pape[8], F.Parodi[12], A.Passeri[41], M.Pegoraro[36], J.Pennanen[14], L.Peralta[21], V.Perevozchikov[43], H.Pernegger[51], M.Pernicka[51], A.Perrotta[5], C.Petridou[47], A.Petrolini[12], H.T.Phillips[38], G.Piana[12], F.Pierre[40], M.Pimenta[21], S.Plaszczynski[19], O.Podobrin[16], M.E.Pol[18], G.Polok[17], P.Poropat[47], V.Pozdniakov[15], M.Prest[47], P.Privitera[39], A.Pullia[28], D.Radojicic[35], S.Ragazzi[28], H.Rahmani[32], J.Rames[11], P.N.Ratoff[20], A.L.Read[33], M.Reale[53], P.Rebecchi[19], N.G.Redaelli[28], M.Regler[51], D.Reid[8], P.B.Renton[35], L.K.Resvanis[3], F.Richard[19], J.Richardson[22], J.Ridky[11], G.Rinaudo[46], I.Ripp[40], A.Romero[46], I.Roncagliolo[12], P.Ronchese[36], V.Ronjin[43], L.Roos[13], E.I.Rosenberg[1], E.Rosso[8], P.Roudeau[19], T.Rovelli[5], W.Ruckstuhl[31], V.Ruhlmann-Kleider[40], A.Ruiz[42], K.Rybicki[17], H.Saarikko[14], Y.Sacquin[40], A.Sadovsky[15], G.Sajot[13], J.Salt[50], J.Sanchez[26], M.Sannino[12], H.Schneider[16], M.A.E.Schyns[53], G.Sciolla[46], F.Scuri[47], Y.Sedykh[15], A.M.Segar[35], A.Seitz[16], R.Sekulin[38], R.C.Shellard[37], I.Siccama[31], P.Siegrist[40], S.Simonetti[40], F.Simonetto[36], A.N.Sisakian[15], B.Sitar[6], T.B.Skaali[33], G.Smadja[25], N.Smirnov[43], O.Smirnova[15], G.R.Smith[38], R.Sosnowski[52], D.Souza-Santos[37], T.Spassov[21], E.Spiriti[41], S.Squarcia[12], H.Staeck[53], C.Stanescu[41], S.Stapnes[33], I.Stavitski[36], G.Stavropoulos[10], K.Stepaniak[52], F.Stichelbaut[8], A.Stocchi[19], J.Strauss[51], R.Strub[9], B.Stugu[4], M.Szczekowski[52], M.Szeptycka[52], T.Tabarelli[28],

O.Tchikilev[43], G.E.Theodosiou[10], A.Tilquin[27], J.Timmermans[31], L.G.Tkatchev[15], T.Todorov[9], D.Z.Toet[31], A.Tomaradze[2], B.Tome[21], L.Tortora[41], G.Transtromer[24], D.Treille[8], W.Trischuk[8], G.Tristram[7], A.Trombini[19], C.Troncon[28], A.Tsirou[8], M-L.Turluer[40], T.Tuuva[14], I.A.Tyapkin[23], M.Tyndel[38], S.Tzamarias[22], B.Ueberschaer[53], S.Ueberschaer[53], O.Ullaland[8], V.Uvarov[43], G.Valenti[5], E.Vallazza[8], J.A.Valls Ferrer[50], C.Vander Velde[2], G.W.Van Apeldoorn[31], P.Van Dam[31], W.K.Van Doninck[2], J.Van Eldik[31], G.Vegni[28], L.Ventura[36], W.Venus[38], F.Verbeure[2], M.Verlato[36], L.S.Vertogradov[15], D.Vilanova[40], P.Vincent[25], L.Vitale[47], E.Vlasov[43], A.S.Vodopyanov[15], M.Voutilainen[14], V.Vrba[11], H.Wahlen[53], C.Walck[45], A.Wehr[53], M.Weierstall[53], P.Weilhammer[8], A.M.Wetherell[8], D.Wicke[53], J.H.Wickens[2], M.Wielers[16], G.R.Wilkinson[35], W.S.C.Williams[35], M.Winter[9], M.Witek[8], G.Wormser[19], K.Woschnagg[49], K.Yip[35], L.Yu[35], O.Yushchenko[43], F.Zach[25], A.Zaitsev[43], A.Zalewska[17], P.Zalewski[52], D.Zavrtanik[44], E.Zevgolatakos[10], N.I.Zimin[15], M.Zito[40], D.Zontar[44], R.Zuberi[35], G.C.Zucchelli[45], G.Zumerle[36]

[1]Ames Laboratory and Department of Physics, Iowa State University, Ames IA 50011, USA
[2]Physics Department, Univ. Instelling Antwerpen, Universiteitsplein 1, B-2610 Wilrijk, Belgium
and IIHE, ULB-VUB, Pleinlaan 2, B-1050 Brussels, Belgium
and Faculté des Sciences, Univ. de l'Etat Mons, Av. Maistriau 19, B-7000 Mons, Belgium
[3]Physics Laboratory, University of Athens, Solonos Str. 104, GR-10680 Athens, Greece
[4]Department of Physics, University of Bergen, Allégaten 55, N-5007 Bergen, Norway
[5]Dipartimento di Fisica, Università di Bologna and INFN, Via Irnerio 46, I-40126 Bologna, Italy
[6]Comenius University, Faculty of Mathematics and Physics, Mlynska Dolina, SK-84215 Bratislava, Slovakia
[7]Collège de France, Lab. de Physique Corpusculaire, IN2P3-CNRS, F-75231 Paris Cedex 05, France
[8]CERN, CH-1211 Geneva 23, Switzerland
[9]Centre de Recherche Nucléaire, IN2P3 - CNRS/ULP - BP20, F-67037 Strasbourg Cedex, France
[10]Institute of Nuclear Physics, N.C.S.R. Demokritos, P.O. Box 60228, GR-15310 Athens, Greece
[11]FZU, Inst. of Physics of the C.A.S. High Energy Physics Division, Na Slovance 2, 180 40, Praha 8, Czech Republic
[12]Dipartimento di Fisica, Università di Genova and INFN, Via Dodecaneso 33, I-16146 Genova, Italy
[13]Institut des Sciences Nucléaires, IN2P3-CNRS, Université de Grenoble 1, F-38026 Grenoble Cedex, France
[14]Research Institute for High Energy Physics, SEFT, P.O. Box 9, FIN-00014 Helsinki, Finland
[15]Joint Institute for Nuclear Research, Dubna, Head Post Office, P.O. Box 79, 101 000 Moscow, Russian Federation
[16]Institut für Experimentelle Kernphysik, Universität Karlsruhe, Postfach 6980, D-76128 Karlsruhe, Germany
[17]High Energy Physics Laboratory, Institute of Nuclear Physics, Ul. Kawiory 26a, PL-30055 Krakow 30, Poland
[18]Centro Brasileiro de Pesquisas Físicas, rua Xavier Sigaud 150, BR-22290 Rio de Janeiro, Brazil
[19]Université de Paris-Sud, Lab. de l'Accélérateur Linéaire, IN2P3-CNRS, Bat 200, F-91405 Orsay Cedex, France
[20]School of Physics and Materials, University of Lancaster, Lancaster LA1 4YB, UK
[21]LIP, IST, FCUL - Av. Elias Garcia, 14-1°, P-1000 Lisboa Codex, Portugal
[22]Department of Physics, University of Liverpool, P.O. Box 147, Liverpool L69 3BX, UK
[23]LPNHE, IN2P3-CNRS, Universités Paris VI et VII, Tour 33 (RdC), 4 place Jussieu, F-75252 Paris Cedex 05, France
[24]Department of Physics, University of Lund, Sölvegatan 14, S-22363 Lund, Sweden
[25]Université Claude Bernard de Lyon, IPNL, IN2P3-CNRS, F-69622 Villeurbanne Cedex, France
[26]Universidad Complutense, Avda. Complutense s/n, E-28040 Madrid, Spain
[27]Univ. d'Aix - Marseille II - CPP, IN2P3-CNRS, F-13288 Marseille Cedex 09, France
[28]Dipartimento di Fisica, Università di Milano and INFN, Via Celoria 16, I-20133 Milan, Italy
[29]Niels Bohr Institute, Blegdamsvej 17, DK-2100 Copenhagen 0, Denmark
[30]NC, Nuclear Centre of MFF, Charles University, Areal MFF, V Holesovickach 2, 180 00, Praha 8, Czech Republic
[31]NIKHEF-H, Postbus 41882, NL-1009 DB Amsterdam, The Netherlands
[32]National Technical University, Physics Department, Zografou Campus, GR-15773 Athens, Greece
[33]Physics Department, University of Oslo, Blindern, N-1000 Oslo 3, Norway
[34]Dpto. Fisica, Univ. Oviedo, C/P. Pérez Casas, S/N-33006 Oviedo, Spain
[35]Department of Physics, University of Oxford, Keble Road, Oxford OX1 3RH, UK
[36]Dipartimento di Fisica, Università di Padova and INFN, Via Marzolo 8, I-35131 Padua, Italy
[37]Depto. de Fisica, Pontificia Univ. Católica, C.P. 38071 RJ-22453 Rio de Janeiro, Brazil
[38]Rutherford Appleton Laboratory, Chilton, Didcot OX11 OQX, UK
[39]Dipartimento di Fisica, Università di Roma II and INFN, Tor Vergata, I-00173 Rome, Italy
[40]Centre d'Etude de Saclay, DSM/DAPNIA, F-91191 Gif-sur-Yvette Cedex, France
[41]Istituto Superiore di Sanità, Ist. Naz. di Fisica Nucl. (INFN), Viale Regina Elena 299, I-00161 Rome, Italy
[42]C.E.A.F.M., C.S.I.C. - Univ. Cantabria, Avda. los Castros, S/N-39006 Santander, Spain, (CICYT-AEN93-0832)
[43]Inst. for High Energy Physics, Serpukov P.O. Box 35, Protvino, (Moscow Region), Russian Federation
[44]J. Stefan Institute and Department of Physics, University of Ljubljana, Jamova 39, SI-61000 Ljubljana, Slovenia
[45]Fysikum, Stockholm University, Box 6730, S-113 85 Stockholm, Sweden
[46]Dipartimento di Fisica Sperimentale, Università di Torino and INFN, Via P. Giuria 1, I-10125 Turin, Italy
[47]Dipartimento di Fisica, Università di Trieste and INFN, Via A. Valerio 2, I-34127 Trieste, Italy
and Istituto di Fisica, Università di Udine, I-33100 Udine, Italy
[48]Univ. Federal do Rio de Janeiro, C.P. 68528 Cidade Univ., Ilha do Fundão BR-21945-970 Rio de Janeiro, Brazil
[49]Department of Radiation Sciences, University of Uppsala, P.O. Box 535, S-751 21 Uppsala, Sweden
[50]IFIC, Valencia-CSIC, and D.F.A.M.N., U. de Valencia, Avda. Dr. Moliner 50, E-46100 Burjassot (Valencia), Spain
[51]Institut für Hochenergiephysik, Österr. Akad. d. Wissensch., Nikolsdorfergasse 18, A-1050 Vienna, Austria
[52]Inst. Nuclear Studies and University of Warsaw, Ul. Hoza 69, PL-00681 Warsaw, Poland
[53]Fachbereich Physik, University of Wuppertal, Postfach 100 127, D-42097 Wuppertal 1, Germany

1 Introduction

This letter reports on a search for orbitally excited B-meson states (B^{**}) in $Z^0 \to b\bar{b}$ decays. $L = 1$ B mesons have not yet been observed experimentally. A possible large production rate of narrow B^{**} mesons in $b-$quark fragmentation has recently attracted attention [1], since it would allow self-tagging flavour identification at production time for studies of neutral B mixing and searches for CP-violation at hadron colliders. Sizable D^{**} production rates have been reported both in B-decays and in $c-$quark fragmentation by ARGUS [2] and CLEO [3], and more recently at LEP by ALEPH [4] and DELPHI [5], thus proving that quark fragmentation is capable of producing primary mesons with orbital excitation. This motivates a search for B^{**} states at LEP.

In the quark model one expects for each spectator flavour four different B meson states with orbital angular momentum $L = 1$ (commonly labeled B^{**} or $B^{**}_{u,d}$ in this paper for $b\bar{u}$ and $b\bar{d}$ states and B^{**}_s for $b\bar{s}$ states). The expected main decay modes of $B^{**}_{u,d}$ mesons are $B\pi$ and $B^*\pi$. In this analysis B and B^* mesons cannot be distinguished, therefore they are labeled as $B^{(*)}$. If the B^{**}_s meson mass is above the $B^{(*)}K$ threshold, this will be the dominant decay mode, since $B_s\pi$ is forbidden by isospin conservation.

Heavy Quark Effective Theory (HQET)[6] groups these four states into two doublets per B-flavour according to the vector sum of the light quark's spin and the orbital angular momentum $j_l = s_q + L$: $j_l = 3/2$; $J^P = 1^+, 2^+$ and $j_l = 1/2$; $J^P = 0^+, 1^+$. The members of the first doublet should be very narrow compared to typical strong decay widths, because only $L = 2$ decays are allowed. This is due to angular momentum and parity conservation for the 2^+ state and a dynamical prediction for the 1^+ partner [6,7]. In the D-meson sector, the two narrow states have been clearly identified experimentally [2,3,8] and spin/parity and decay characteristics have been shown to be in accord with the HQET predictions.

A measurement of production of B^* mesons in Z decays has been performed by the DELPHI [9] as well as L3 [10] and ALEPH [11] collaborations. The B^*/B production rate and the B^* polarization ratio σ_T/σ_L have been found to be compatible with the spin counting expectations 3:1 and 2:1. In these measurements the signal was obtained in the $B\gamma - B$ mass difference spectrum, using specially developed inclusive B reconstruction methods. The DELPHI method serves as the basis for B^{**} reconstruction in this paper.

The DELPHI detector is capable of studying B^{**} production by using inclusively reconstructed B mesons and pion tracks originating from the primary vertex. The precise vertex reconstruction capability of DELPHI makes it possible to efficiently tag $b\bar{b}$ events. In the analysis that follows, an enriched sample of $b\bar{b}$ events from the 1991, 1992 and 1993 LEP runs is used. The B momentum in each hemisphere is reconstructed in an inclusive fashion, and it is combined with additional pions coming from the primary vertex to form the $B^{(*)}\pi$ signal. Measurements are presented for the mean Q-value of transitions between $L = 1$ and ground state B-mesons as well as the $B^{**}_{u,d}$ production rate per $b-$jet. The signal is interpreted in the framework of quark model predictions.

2 The DELPHI Detector and Event Selection

DELPHI is a 4π detector with emphasis on particle identification, three dimensional reconstruction, high granularity and precise vertex information. A complete description can be found in reference [12]. The detectors most relevant to this study are the tracking chambers (Vertex Detector, Inner Detector, Time Projection Chamber and Outer Detector) and the barrel electromagnetic calorimeter (High-density Projection Cham-

ber). DELPHI's vertex detector consists of three concentric shells of Si-strip detectors in the central region at radii of 6.3, 9 and 11 cm parallel to the beam pipe for precision reconstruction near the interaction region. The algorithm that is used to enhance the $b\bar{b}$ content, as well as the algorithm used to define the candidate track from the primary vertex for the B^{**} decay, rely on good vertex reconstruction. Therefore, the analysis is restricted to the barrel region ($45° < \theta < 135°$) where there is complete vertex detector coverage. Inclusive reconstruction of the B momentum is based on charged and neutral particle reconstruction. The alignment of the various tracking detector components as well as an accurate description of efficiencies, resolutions and covariance matrix elements of charged tracks, which are crucial for the present analysis, have been monitored and adjusted using $Z^0 \to \mu^+\mu^-$ decays and primary vertex fits of non-$b\bar{b}$ hadronic events. A momentum resolution of $\sigma(p)/p = 0.0011 \cdot p(GeV/c)$ is achieved for muon pairs in the barrel region. Photons and π^0's that are reconstructed by the High-density Projection Chamber (HPC) have a $\sigma(E)/E = 0.26/\sqrt{E} \oplus 0.046$ and an angular resolution of around 0.002 rad in the azimuthal angle ϕ and the polar angle θ.

Using standard barrel hadronic selection [13], including a cut on the polar angle of the thrust axis ($|\cos\Theta_{thrust}| < 0.7$), 1 026 793 events are selected from the 1991, 1992 and 1993 data. In order to enrich the sample in $b\bar{b}$ events, a B meson tagging algorithm exploiting the large B lifetime [14,15] is applied. A probability is calculated for each event assuming that all the well-measured tracks originate from a primary vertex compatible with the beam spot. Selecting only those events where this probability is less than 1% results in an efficiency of $65 \pm 3\%$ and a purity of $84 \pm 4\%$ for $b\bar{b}$ events. This beauty enhanced sample consists of 175 960 events.

Efficiencies, backgrounds and resolutions are calculated with the DELPHI simulation package, DELSIM, which uses the JETSET 7.3 Monte Carlo generator [16] with parameter adjustments from previous QCD studies [17]. The $B^* - B$ mass difference in the JETSET generator was fixed to the current Particle Data Group world average. In addition, special Monte Carlo samples including production and decay of B^{**} mesons have been generated using masses, widths and decay modes as predicted by HQET [18].

3 Inclusive B reconstruction

The B meson momentum is reconstructed using the same algorithm [19] that is used in the DELPHI B^* analysis [9]. The events are divided into hemispheres defined by the thrust axis. The rapidity of each reconstructed charged (assuming pion mass) and neutral particle (assuming photon mass) with respect to the thrust axis is calculated. The particles whose rapidities are outside a window of ± 1.5 units are considered to be B meson decay products. The momenta of these particles are added together in each hemisphere to arrive at a B meson momentum estimate for each side of the event. This raw B energy is corrected by using the reconstructed raw invariant mass m_y and the ratio of the energy seen in the hemisphere to the beam energy ($x_h = E_{hemisphere}/E_{beam}$). The invariant mass is set to the current mass value for the B meson [8]. Details of this procedure can be found in [9]. To reduce the amount of badly reconstructed B-mesons a minimum reconstructed energy of 20 GeV in the rapidity gathering algorithm is required, and the reconstructed mass has to lie within ± 2.5 GeV/c^2 of the mean reconstructed B meson mass. This algorithm is only meaningful in two jet events and for the most energetic jet in three jet events. These have been identified using the LUCLUS algorithm [16] with a transverse momentum cutoff of 3.5 GeV/c.

Using the simulation sample, the energy resolution of this inclusive technique is determined to be 7% for 70% of the B mesons (the rest constitute a non-Gaussian tail towards higher estimated energies); the angular resolutions in θ and ϕ can be parameterized as double Gaussians with widths 0.015 rad for 60% of the data and 0.038 rad for the remaining 40%. The inclusive rapidity distributions for charged and neutral particles as well as the distributions of reconstructed B mass and reconstructed B energy observed in the data agree very well with the Monte Carlo expectations [9]. The simulation prediction of the resolutions of the inclusive B reconstruction algorithm is verified by the good agreement in the width of the $B^* \to B\gamma$ mass difference peak [9].

4 Experimental Procedure and Results

If the mass of B^{**} mesons is above the $B^*\pi$ but below the $B\rho$ threshold, B^{**} mesons mainly decay into $B\pi$ or $B^*\pi$. Parity conservation restricts the expected main decay modes of the single states: the spin-parity state 0^+ would decay into $B\pi$ (s-wave), the two 1^+ states into $B^*\pi$ (s- or d-wave), and the 2^+ state into both $B\pi$ and $B^*\pi$ (both d-wave). Positively charged pions can come from decays of the $I_3 = +1/2$ states B^{**+} (containing a $\bar{b}$-quark) and $\bar{B}^{**0}$ (containing a b-quark). Therefore, flavour tagging with e.g. inclusive leptons or jet charge cannot be used to enhance the ratio of B^{**} signal to background.

Both the B decay particles as well as the B^{**} decay pion have large rapidities. However, since the B^{**} decays strongly, the pion should originate from the primary vertex and not from the B decay vertex.

The quantity which is best accessible experimentally with inclusive B reconstruction methods is the Q-value of the decay:

$$\mathrm{Q} = m(B^{(*)}\pi) - m(B^{(*)}) - m(\pi) \equiv m(B^{**}) - m(B^{(*)}) - m(\pi).$$

The symbol $B^{(*)}$ denotes both B and B^* states, which cannot be distinguished with the present method. The resolution of the present method can be parameterized as $\sigma(\mathrm{Q}) = 18\ \mathrm{MeV/c^2} + 65\ \mathrm{MeV/c^2} \times (\mathrm{Q}\ [\mathrm{GeV/c^2}])$. It is dominated by the energy and angular resolution of the B-meson. Whether the decay was actually into B or B^* and whether the B^* decay photon has been reconstructed, only has a negligible effect on the resolution in the Q-value. However, the decay of a B^{**} of a given mass to a $B^*\pi$ gives rise to a Q-value which is shifted downwards by the B^*-B mass difference of 45 $\mathrm{MeV/c^2}$ compared to the Q-value of a $B\pi$ decay. Therefore, for the determination of a B^{**} mass from the measurable Q-value, an assumption about the B^*/B ratio in the signal has to be employed.

Pion tracks are selected which are compatible with the primary vertex and not with a secondary B decay vertex. This is accomplished by the following algorithm. All well measured tracks with at least two vertex detector hits associated are classified into three vertices: the primary vertex which has to be compatible with the known beam spot, and two B decay vertices. The rapidity classification serves as a starting point: all particles with $|y| < 1.5$ are assigned to the primary vertex, and those with $y < -1.5$ and $y > 1.5$ to the two secondary vertices. Three vertex fits are then performed. The track contributing the largest χ^2 is then tried at the other kinematically allowed vertex (i.e. the primary vertex if it was a secondary before and vice versa). The new vertex distribution is accepted if the χ^2 gets better, otherwise the old distribution is kept. If the track gives the largest χ^2 contribution in both situations, it is discarded. This procedure is continued until no

track gives a χ^2 contribution larger than 4. For the B^{**} pion candidates, only tracks fitted to the primary vertex are accepted.

In order to get a clear distinction between primary and secondary vertices, the reconstructed decay length (in the signal hemisphere) is required to exceed 1.5 mm. A further reduction of tracks from B decays can be achieved by requiring a value of less than 1% for the probability that all the particles in the signal hemisphere stem from the primary vertex. An additional selection is performed on the lifetime-signed impact parameter of the pion candidate tracks: if the lifetime-signed impact parameter of the candidate pion with respect to the primary vertex is positive, then the χ^2 probability that it originates from the primary vertex has to be larger than 15%.

The distribution of the measured $B^{(*)}\pi$ Q-values is shown as data points in figure 1a. There is a large excess of combinations on top of a smoothly falling background. The background is well described by the Monte Carlo prediction, in which B^{**} decay pions have been suppressed, shown as shaded area in figure 1a. The Monte Carlo statistics is comparable to the data statistics. Figure 1b shows the difference plot, which is fit to a simple Gaussian with central value

$$\mathrm{Q}(B^{**} \to B^{(*)}\pi) = 284 \pm 5\,(\mathrm{stat.}) \pm 15\,(\mathrm{syst.})\ \mathrm{MeV/c^2}$$

and Gaussian width

$$\sigma = 79 \pm 5\,(\mathrm{stat.}) \pm 8\,(\mathrm{syst.})\ \mathrm{MeV/c^2}$$

containing

$$N = 2157 \pm 120\,(\mathrm{stat.}) \pm 323\,(\mathrm{syst.})$$

events. This corresponds to a statistical significance of 18 standard deviations. Systematic uncertainties dominate in the measurements of all these quantities. They were determined by modifying cuts and by fitting different background shapes (originating from simulation and various phenomenological background models) to the data. Employing the simulation prediction for the background shape, the normalization had to be adjusted by the factor $0.95 \pm 0.01\,(\mathrm{stat.}) \pm 0.04\,(\mathrm{syst.}$, dependence on cuts) in order to describe the data well at large Q-values.

Possible reflections from $B_s^{**} \to B^{(*)}K$ decays are expected to contribute in the Q-value range between 50 and 250 MeV/c^2 at the level of 10% to the expected $B_{u,d}^{**}$ signal. Additional uncertainties are introduced by the possible production of $\Sigma_b \to \Lambda_b\pi$ and reflections from the decay $B_{u,d}^{**} \to B^{(*)}\rho$. Their possible influence has been considered in evaluating the systematic errors.

To check whether the signal could be an artifact of the employed vertex procedure, the selection cuts were varied within wide ranges. Also using simple analysis techniques without vertex fitting, a clear excess with the same characteristics is observed, but on top of a larger combinatorial background.

Furthermore the charge symmetry of the signal was tested by dividing the sample according to positive and negative pion charge, positive and negative jet charge, and positive and negative product of jet and pion charge. The jet charge was defined as $(Q_{jet,same} - Q_{jet,oppo})$, where the Q_{jet} were calculated using $Q_{jet} = \sum_i Q_i \cdot p_i^{0.6} / \sum_i p_i^{0.6}$ in the signal hemisphere (excluding the candidate pion) and in the opposite hemisphere. In all these cases the rates are compatible with the Monte Carlo prediction.

All tests have been passed successfully, no cut being found where the behaviour of the data was different from that expected from the simulation prediction for a strongly decaying isospin 1/2 $B^{(*)}\pi$ resonance.

The total B_{ud}^{**} rate is determined to be

$$\sigma_{B_{u,d}^{**}}/\sigma_{b-jet} = 0.27 \pm 0.02\,(\mathrm{stat.}) \pm 0.06\,(\mathrm{syst.}).$$

In this rate calculation it was assumed that 2/3 of all B^{**} decay into charged pions and 1/3 into (unobserved) π^0, according to isospin rules for an $I = 1/2$ decay into an isovector and an isospinor. Different cuts on the B reconstruction quality and the candidate pion selection have been used. The largest systematic uncertainty (± 0.03) was observed when dividing the event sample into two hemispheres defined by the angle of the pion in the B^{**} rest frame with respect to the B^{**} flight direction (helicity angle). Including the limited Monte Carlo statistics, the systematic error of the acceptance calculation is estimated to be $\pm 15\%$.

From this the total number of $B^{**}_{u,d}$ mesons per hadronic Z decay is determined to be

$$N_{B^{**}_{u,d}}/Z_{had} = 0.118 \pm 0.007\,(\text{stat.}) \pm 0.023\,(\text{syst.}).$$

Assuming the b-baryon rate to be $10 \pm 4\,\%$ and the $B_s^{(*)}$ rate to be $13 \pm 2\,\%$, the relative amount of $B_{u,d}$ mesons which originate from $B^{**}_{u,d}$ decay is

$$\sigma_{B^{**}_{u,d}}/\sigma_{B_{u,d}} = 0.35 \pm 0.02\,(\text{stat.}) \pm 0.08\,(\text{syst.}).$$

5 Interpretation of the signal

If the signal were due to a single very narrow resonance, the expected Gaussian width would be around $\sigma = 38$ MeV/c^2, as shown in figure 2a. This can clearly be excluded. In order to describe the much broader observed signal with a single resonance, its full width would have to be

$$\Gamma = 145 \pm 28 \text{ MeV/c}^2.$$

The signal would be broadened if different resonances with different masses contribute, and some decay into $B\pi$ and others into $B^*\pi$, leading to a 45 MeV/c^2 shift in Q-value. The observed signal shape is consistent with predictions for orbital excitations [18]. According to this model the signal would consist of two narrow (1^+ and 2^+) and two broad (0^+ and 1^+) resonances of roughly the same mass (splittings at the 10 MeV/c^2 level), decaying into $B^*\pi$ or $B\pi$, as dictated by spin-parity rules. The 2^+ is predicted to decay into both $B^*\pi$ and $B\pi$ with about equal rates.

There is no prediction about the relative production rates of the four B^{**} states, but reasonable assumptions range between 5:3:3:1 (spin counting) and 1:1:1:1 (state counting) for the $2^+ : 1^+ : 1^+ : 0^+$ states. In the D meson sector the production ratio of $D_2^* \to D\pi$ to $D_2^* \to D^*\pi$ to $D_1 \to D^*\pi$ has been measured by CLEO [3] to be roughly 2:1:3. This is compatible with the state counting picture for the narrow states. It also confirms the $D_2^* \to D\pi : D_2^* \to D^*\pi = 1.8 : 1$ decay branching ratio prediction from HQET [18]. These facts motivate the use of state counting and HQET predictions.

An interpretation of the signal as stemming from *only* narrow resonances (of width $\Gamma \approx 20$ MeV/c^2) is unlikely. If the mass splitting were small, the observable signal width would be only 46 MeV/c^2; for splittings in the order of 35 MeV/c^2 (as in the D meson sector) it is expected to be 52 MeV/c^2. To achieve a signal with the observed width, a splitting of 80 MeV/c^2 would be necessary, as shown in figure 2b. In this case, the experimental resolution should start to resolve a substructure. The expectation for this model does not describe the data well. Also, such a large splitting is not expected [18]. Therefore the observed signal should also contain broad resonances with a full width Γ of about 150 MeV/c^2.

The data is compared to a model based on masses and widths for the narrow states as predicted from the HQET model of Eichten et al. [18]. Further assumptions are that the

two broad states have a width of 150 MeV/c^2 and that the four B^{**} states are produced in a ratio of 1 : 1 : 1 : 1. Assuming the broad resonances to have the same mass as the narrow ones does not describe the data well; therefore they have been shifted downwards by 50 MeV/c^2 and their rate has been increased by 50% for figure 2c. Such an energy splitting between the $j_l = 3/2$ and 1/2 states has been proposed by Rosner [7]. The agreement between data and simulation would be better by slightly lowering the masses of the narrow states.

Assuming a $B^*\pi$ to $B\pi$ ratio of 2 : 1, the mean mass difference between the B meson and the cross section weighted mean of the four expected $B^{**}_{u,d}$ resonances is determined to be $M(B^{**}_{u,d}) - M(B_{u,d}) = 453 \pm 5\,(\text{stat.}) \pm 20\,(\text{syst.})$ MeV/c^2, corresponding to a mass

$$M(B^{**}_{u,d}) = 5732 \pm 5\,(\text{stat.}) \pm 20\,(\text{syst.})\ \text{MeV}/c^2.$$

Part of the systematic error is due to the uncertainty in the ratio of decays into B^* and B in the mapping from Q-value to mass difference; it can accommodate for the two reasonable assumptions 1 : 1 and 3 : 1. This value is consistent with the predicted 488 MeV/c^2 for the $B^*_2 - B$ and 476 MeV/c^2 for the $B_1 - B$ mass differences[18].

Figure 2d is an attempt to describe the data without a large mass splitting between narrow and broad states. In this case, the mean mass difference as determined above and a mass splitting between the narrow states of 20 MeV/c^2 is used. The ratio of the broad to narrow states is 3:2, an even larger contribution of the broad states would make the agreement better.

With the current experimental sensitivity the interpretations in figure 2c and d cannot be distinguished, neither can one of them be discarded. The simple Gaussian fit shown in figure 1b describes the data best. However, due to the large freedom, consistent results can be achieved in a number of possible scenarios based on quark model and HQET.

6 Summary and Conclusions

Strong experimental evidence for the existence of orbitally excited B-mesons ($B^{**}_{u,d}$) has been obtained from the $B^{(*)}\pi$ Q-value distribution using an inclusive B reconstruction method and separating primary and secondary vertices with the DELPHI silicon vertex detector.

The $B^{(*)}\pi$ Q-value distribution shows a large signal at Q = 284 $\pm$ 5 (stat.) $\pm$15 (syst.) MeV/c^2 with a Gaussian width of $\sigma(\text{Q}) = 79 \pm 5\,(\text{stat.}) \pm 8\,(\text{syst.})$ MeV/c^2. The signal can be described as a single resonance of mass m = 5732 $\pm$ 5 (stat.) $\pm$ 20 (syst.) MeV/c^2 and full width Γ = 145 $\pm$ 28 MeV/c^2. It can also be interpreted as stemming from several narrow and broad predicted $B^{**}_{u,d}$ resonances, as predicted by quark models and HQET and observed in the D meson sector. The rate of $B^{**}_{u,d}$ mesons per b-jet is 0.27 $\pm$ 0.02 (stat.) $\pm$ 0.06 (syst.).

In conclusion, the existence of orbitally excited B mesons has been experimentally established. The results are in general agreement with predictions.

During the process of refereeing we learned about a paper by the OPAL Collaboration [20] which also shows evidence for B^{**} production.

Acknowledgements

We are greatly indebted to our technical collaborators and to the funding agencies for their support in building and operating the DELPHI detector, and to the members of the CERN-SL Division for the excellent performance of the LEP collider.

References

[1] M. Gronau, A. Nippe and J.L Rosner, Phys. Rev. **D 47** (1993) 1988

[2] ARGUS Collaboration, H. Albrecht et al., Phys. Lett. **B 221** (1989) 422
ARGUS Collaboration, H. Albrecht et al., Phys. Lett. **B 232** (1989) 398

[3] CLEO Collaboration, P. Avery et al., Phys. Rev. **D 41** (1990) 774
CLEO Collaboration, P. Avery et al., Phys. Lett. **B 331** (1994) 236
CLEO Collaboration, F. Butler et al.,*Observation of* $D_1(2430)^+$ *and* $D_2^*(2470)^+$, contributed paper to the International Conference on High Energy Physics, Glasgow 1994, ref. gls0185

[4] ALEPH Collaboration, D^{**} *Production in* Z^0 *Decays*, contributed paper to the International Conference on High Energy Physics, Glasgow 1994, ref. gls0577

[5] DELPHI Collaboration, *Study of D,* D^* *and* D^{**} *Production in* Z^0 *Hadronic Decays*, contributed paper to the International Conference on High Energy Physics, Glasgow 1994, ref. gls0185

[6] N. Isgur, M.B. Wise, Phys. Lett. **B 232** (1989) 113;
M.B. Wise, Procs. XVI International Symposium on Lepton and Photon Interactions, Ithaca, New York, 1993, Ed. P. Drell, D. Rubin, p. 253.

[7] J.L. Rosner, Comm. Nucl. Part. Phys. **16** (1986) 109

[8] Particle Data Group, Phys. Rev. **D 50** (1994) 1173

[9] DELPHI Collaboration, DELPHI Note 94-80 Phys 397; contributed paper to the International Conference on High Energy Physics, Glasgow 1994, ref. gls0305; DELPHI draft 103, to be published

[10] L3 Collaboration, M. Acciarri et al., CERN-PPE/94-143 (1994)

[11] ALEPH Collaboration, *A study of* B^* *Production in Z Decays*, contributed paper to the International Conference on High Energy Physics, Glasgow 1994, ref. gls0598

[12] DELPHI Coll., P. Aarnio et al., Nucl. Instr. Meth. **A 303** (1991) 233-276

[13] DELPHI Coll., P. Abreu et al., Z. Phys. **C 54** (1992) 55

[14] ALEPH Coll., D. Buskulic *et al.*, Phys. Lett. **B 313** (1993) 535

[15] DELPHI Coll., P. Abreu et al., CERN-PPE-94-131

[16] T. Sjöstrand, Comp. Phys. Comm. **39** (1986) 347;
T. Sjöstrand and M. Bengtsson, Comp. Phys. Comm. **43** (1987) 367

[17] W. de Boer, H. Fürstenau, *Comparison of DELPHI data with QCD models*, Delphi Note 91-75 Phys 129

[18] E.J. Eichten, C.T. Hill and C. Quigg, Phys. Rev. Lett. **71** (1993) 4116

[19] O. Podobrin, *An algorithm for inclusive B hadron reconstruction*, DELPHI note, in preparation

[20] OPAL Coll., R. Akers et al., CERN-PPE-94-206

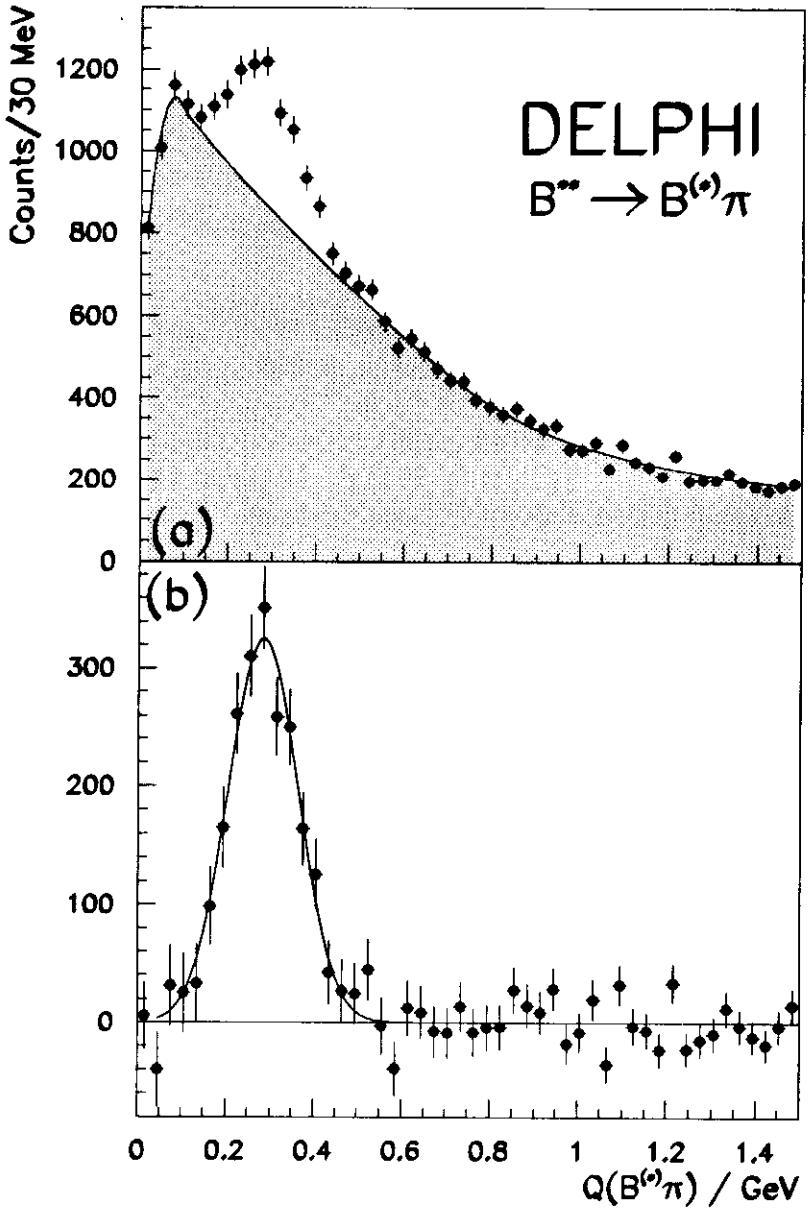

Figure 1: (a) Distribution of the Q-value of $B^{(*)}\pi$ pairs (data points) along with the Monte Carlo expectation without B^{**} production (shaded area). Q is defined as $Q=m(B^{(*)}\pi) - m(B^{(*)}) - m(\pi)$. (b) Background subtracted $B^{(*)}\pi$ pair Q-value distribution. The fit is a simple Gaussian.

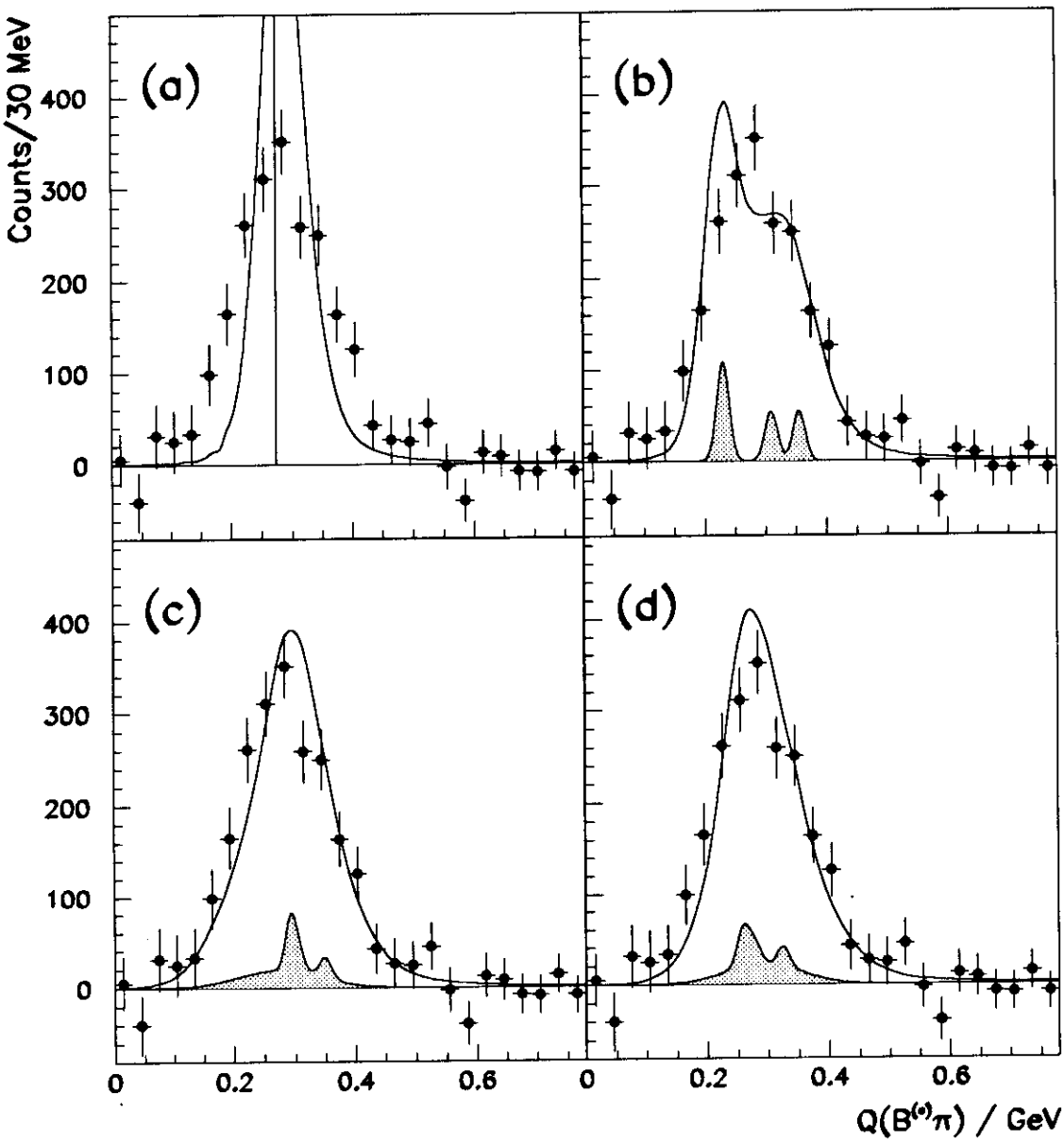

Figure 2: Comparison of the background subtracted Q-value distribution (data points) with various models (solid line). The shaded area corresponds to the generated distribution (scaled by a factor 0.2) prior to detector resolution effects : (a) a delta-function at Q = 284 MeV/c^2 (detector resolution including non-Gaussian tails). (b) two narrow resonances, one decaying into $B\pi$, the other equally into $B\pi$ and $B^*\pi$. A mass splitting of 80 MeV/c^2 is necessary to describe the observed width. (c) the model of Eichten et al. [18], plus broad resonances shifted downwards by 50 MeV/c^2. (d) two narrow and two broad states without large mass splitting.